A multi-element THz imaging system

Eichhorn, Finn; Høgstedt, Lasse; Buron, Jonas Christian Due; Olsson, Rasmus Kjelsmark; Kusk, Anders; Dall, Jørgen; Jepsen, Peter Uhd

Published in:
35. International Conference on Infrared Millimeter and Terahertz Waves

Link to article, DOI:
10.1109/ICIMW.2010.5612544

Publication date:
2010

A multi-element THz imaging system

Finn Eichhorn[a], Lasse Høgstedt[a], Jonas C. D. Buron[a], Rasmus K. Olsson[a], Anders Kusk[b], Jørgen Dall[b], and Peter U. Jepsen[a]

[a]DTU Fotonik, Technical University of Denmark, DK-2800 Kgs. Lyngby, Denmark

[b]DTU Space, Technical University of Denmark, DK-2800 Kgs. Lyngby, Denmark

***Abstract*— We report on a broadband multi-element THz imaging system based on fiber-coupled, integrated photoconductive emitters and detectors. 32 detectors and 32 emitters are arranged in a planar array. Advanced image reconstruction algorithms are employed to reconstruct an object in the imaging plane.**

I. Introduction And Background

THz imaging is today largely carried out by time-consuming raster-scanning techniques [1]. The main concept of our broadband multi-element THz imaging system is inspired by phased array and synthetic aperture radar imaging systems operating in the microwave range. Combining the large knowledge on data analysis and imaging capabilities of these systems in a new multi-element THz system will give a novel possibility of fast image acquisition, thus avoiding time-consuming raster scanning. Our system features an in-plane emitter-detector array consisting of 32 emitters and 32 receiver units (see Figure 1).

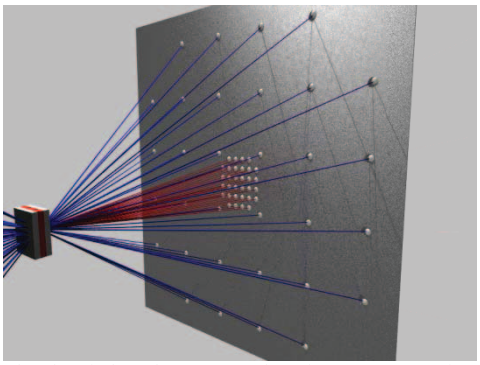

Figure 1: Sketch of the planar array imaging structure of emitters and detectors illuminating a target. The emitters are radiating towards the target along the blue lines and the detectors are receiving the scattered radiation from the target (red lines). The emitter and detector spacings ensure the best possible resolution without introducing ambiguities/grating lobes.

The technology used in every single unit is inherited from the standard THz-TDS systems making use of photoconductive switches driven by a femtosecond laser pulse train. A novel concept is the all-fiber laser pulse delivery network. By avoiding all free-space optics, including a free-space dispersion compensation unit, the system wins on robustness, which is of great importance for making the step from the laser laboratories and towards real life imaging applications.

II. Results

It is a nontrivial task to distribute femtosecond high power laser pulses to 32 THz emitters and 32 detectors via optical fiber. We have designed a fiber link [2], in which the laser pulses are first stretched, then split into 32 channels and finally compressed to approximately 100 fs duration when they reach the emitters and detectors, in order to obtain efficient terahertz generation. The advantage of an all-fiber design is a system that is very stable with respect to external vibrations and temperature fluctuations. The different fibers and fiber components are spliced together using fusion splicing and no further alignment is then needed.

When a laser pulse propagates in an optical fiber it will be either stretched or compressed depending on the dispersion of the fiber and nonlinear effects become an issue. In order to handle the high optical power and to keep the peak power low we first stretch the pulse for as large a fraction of the fiber link as possible. We do this by stretching the output of the fiber lasers in a dispersion compensating fiber (DCF) module from OFS Fitel (EWBDK) with normal dispersion. Figure 2 shows a sketch of the fiber link of a pulse distribution setup, delivering short pulses to either the emitter or detector array. The normal dispersion of the DCF is compensated by the anomalous dispersion of the standard single-mode fiber (SMF). The stretched laser pulse was split into 32 equal portions in a 1 × 32 power splitter before it was recompressed to a FWHM pulse length of sub-100 fs [2].

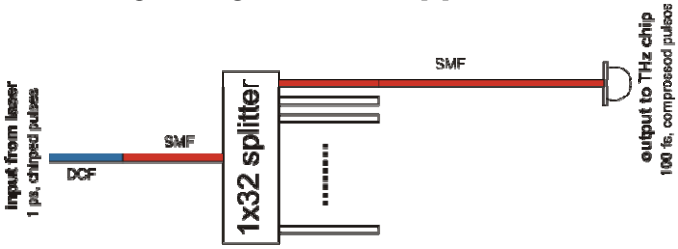

Figure 2 Fiber link for the delivery of sub-100 fs compressed pulses to fiber coupled photoconductive emitters and detectors. DCF (blue) – Dispersion compensated fiber (normal dispersion), SMF – Single mode fiber (red) (anomalous dispersion).

The laser system delivering pulses to the fiber link is a dual-femtosecond fiber-based laser system from Toptica Photonics AG with approximately 4.0 nJ per laser, 1-ps laser pulses around 1550 nm with a 90-MHz pulse repetition rate. The two femtosecond lasers are locked to the same repetition rate by an active control, and the relative time delay can be adjusted

electronically between 0.0–1.0 ns This feature enables electronically controlled optical sampling (ECOPS).

Figure 3 shows an autocorrelation of the pulses compressed in the fiber link setup sketched in Figure 2. The pulses are here launched from one of the two lasers of the system into the fiber link and the measured FWHM of the autocorrelation is 99 fs (~ 80 fs pulse length). The pulse energy of the initial 1 ps laser output pulse is here 3.25 nJ and the pulse energy after the splitter is 0.06 nJ (corresponding to 5 mW average power). The optimal fiber link length e.g. shortest pulse length is investigated by a fiber cut-back measurement.

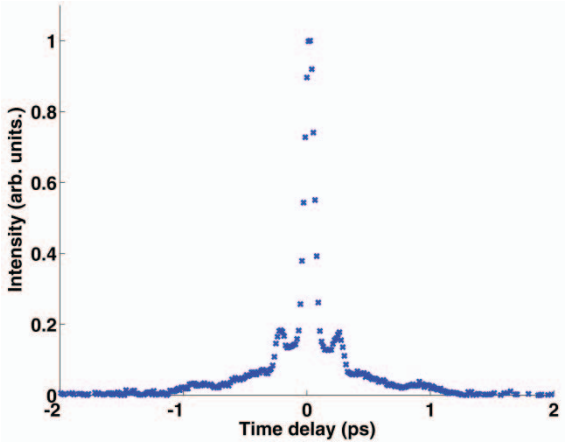

Figure 3 Measured autocorrelation of the compressed pulse at the end of the fiber link. The FWHM of the autocorrelation is 99.2 fs ~70 fs pulse length.

The THz antennas are low temperature-grown InGaAs-based photoconductive switches designed for 1550 nm [3]. The material is commercially available from Menlo Systems GmbH. A generated and detected THz pulse in the time domain and in the frequency domain from the all-fiber system is depicted in Figure 4. The THz transient has a near-single-cycle appearance in the time domain, and a corresponding smooth frequency spectrum spanning the range 0.1-2 THz.

The spectral amplitude of the generated THz signal has a peak dynamic range of approximately 100, corresponding to 40-dB dynamic range in power. The measurement was done by lock-in detection and chopping of the bias voltage on the emitter at a frequency of 1 kHz.

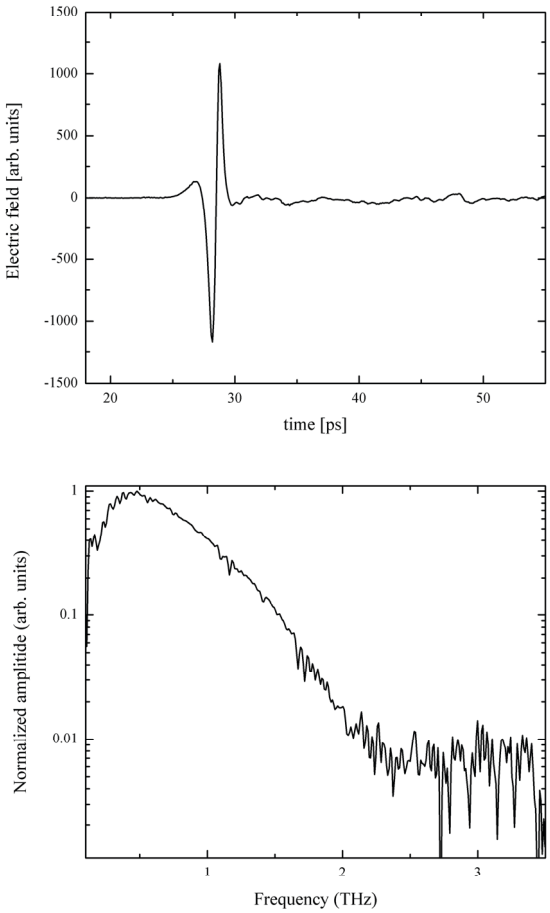

Figure 4 (top) THz pulse in the time domain and (bottom) its frequency spectrum generated and detected in photoconductive switches excited by compressed pulses from the fiber link.

The generated THz radiation is collimated out of the THz antenna by an integrated substrate lens and directed towards a target 0.3 m away from the emitter/detector plane.

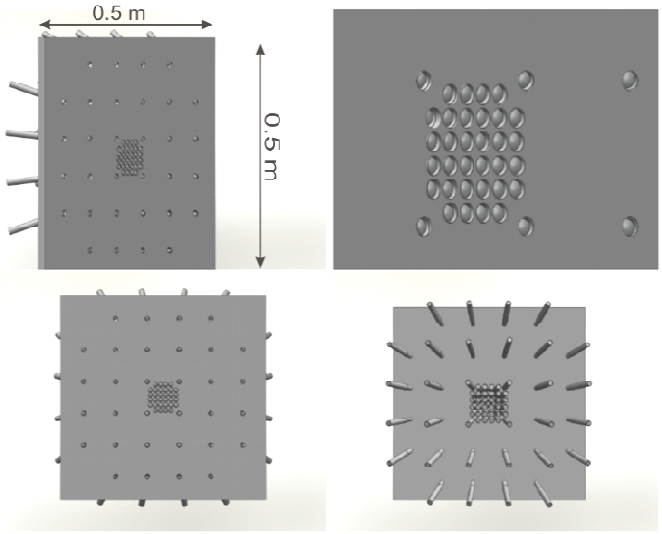

Figure 5 3-D rendering of the realized antenna mounting structure for the planar array. The receivers are stacked in the inner part spaced by 13 mm and the transmitters are in the outer part spaced by 80 mm.

Figure 5 shows a sketch of how the 32 receivers are stacked in a 6 × 6 grid (corners omitted due to the availability of fiber splitters) in the inner part of the array and spaced by 13 mm. The transmitter units are placed in the outer part and spaced by 80 mm. All units are fitted into a 20 mm × 500 mm × 500 mm aluminum mounting structure and pointing towards a center of scene at 0.3 m from the structure.

The array in Figure 5 is implemented as a multistatic radar that transmits sequentially on each of the TX antennas and receives the scattered signal simultaneously on each of the RX antennas. For a target in the far-field, each TX-RX element pair provides the same signal as would be provided by an equivalent monostatic element at the midpoint between the TX and RX elements. Hence, the element layout in Fig. 5 ensures an equidistant multistatic element spacing of about half the physical RX spacing and an effective aperture size of about half the physical TX aperture size.

In the cross-range direction, a passive diffraction-limited system would offer an angular resolution of

$$\alpha = \frac{\lambda}{D} \tag{1}$$

where λ is the wavelength of the incident radiation and D is the diameter of the aperture. The spatial cross-range resolution is found by multiplying (in radians) with the range to the object. For an active monostatic system, the angular resolution is half of that in (1) [4], whereas, for a multistatic system like that in Fig. 5, (2) holds true for an object in the far field, as the effective size of the aperture is half the size of the transmitter aperture.

The angular ambiguity spacing θ depends on the effective element spacing d

$$\theta = \frac{\lambda}{d} = \frac{\lambda N}{D} \tag{2}$$

where N is the effective number of elements. Hence, large objects call for closely spaced elements. Equation (2) applies to a multistatic system, for which the ambiguity spacing is twice that of a monostatic radar system [5], as its effective elements spacing is half of the physical element spacing.

The scattered THz transients are detected in a parallel fashion at the positions of the 32 detectors, and an image is reconstructed using back-projection techniques, implemented on a graphics processing unit for real-time operation. A simulated reconstruction is shown in Figure 6. The simulation is performed for a Gaussian pulse system with a bandwidth of 900 GHz centered around a frequency of 550 GHz. The 3-dB cross-range resolution is 0.4 mm and the first ambiguities are centered approximately 5 mm from the point target. The ambiguities are smeared due to the large bandwidth and are 20 dB below the peak. The reconstruction algorithms used allows focusing in a full volume of 2 cm (range) × 4 cm × 4 cm.

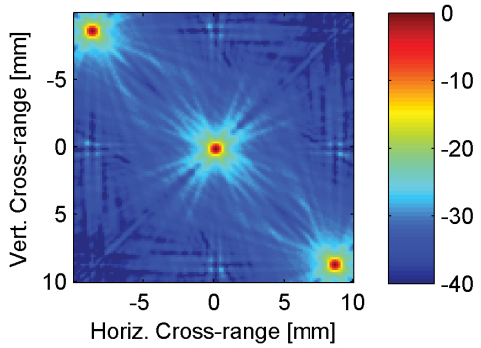

Figure 6: Cross-range slice of 3 simulated point targets, reconstructed with back-projection. Color scale is decibel relative to peak amplitude

We will show the recent progress towards this experimental THz imaging system.

REFERENCES

[1] W. L. Chan, J. Deibel, and D. M. Mittleman, "Imaging with terahertz radiation," Rep. Prog. Phys., vol. 70, pp. 1325–1379, 2007.

[2] F. Eichhorn, R. K. Olsson, J. C. D. Buron, L. Grüner-Nielsen, J. E. Pedersen, and P. U. Jepsen, "Optical fiber link for transmission of 1-nJ femtosecond laser pulses at 1550 nm," Opt. Express, vol. 18, pp. 6978-6987, 2010.

[3] B. Sartorius, H. Roehle, H. Künzel, J. Böttcher, M. Schlak, D. Stanze, H. Venghaus, and M. Schell, "All-fiber terahertz time-domain spectrometer operating at 1.5 μm telecom wavelengths," Opt. Express, vol. 16, pp. 9565-9570, 2008.

[4] W. G. Carrara, R. S. Goodman, and R. M. Majewski, Spotlight Synthetic Aperture Radar: Signal Processing Algorithms. Norwood, MA: Artech House, 1995.

[5] D. A. Ausherman, A. Kozma, J. L. Walker, H. M. Jones, and E. C. Poggio, "Developments in radar imaging," IEEE Trans. Aerosp. electron. Syst., vol. AES-20, no. 4, pp. 363–400, Jul. 1984